Some ethinylquinoxalines as corrosion inhibitors of steel in hydrochloric acid

A.G. Berezhnaya,* V.V. Chernyavina, I.I. Krotkii and A.V. Gulevskaya

Southern Federal University, ul. Zorge 7, 344090 Rostov-on-Don, Russian Federation
**E-mail: berezhnaya-aleksandra@mail.ru*

Abstract

The protective effect of 2-chloro-3(*p*-tolylethynyl)quinoxaline (I), 2,3-bis((4-methoxyphenyl)-ethynyl)quinoxaline (II), 2-(4-methoxyphenyl)-3-(*p*-tolylethynyl)quinoxaline (III) and 2,3-bis(phenylethynyl)quinoxaline (IV) as inhibitors of acid corrosion of low-carbon steel (St3) in 1 M hydrochloric acid in the temperature range of 25–80°C has been studied. At a temperature of 25°C and a concentration of 0.1 mmol/l, the protective effect of the ethynylquinoxaline derivatives ((I–IV)) was found to be 82–92% depending on the structure. When the temperature increases to 60°C, the efficiency decreases to 35–57%. The studied compounds increase the value of the effective activation energy of corrosion and block a fraction of the steel surface upon adsorption. It is shown that the adsorption of the studied ethynylquinoxaline derivatives is described by the Langmuir isotherm. It has been established that compounds I and II are characterized only by chemical adsorption, while compounds III and IV exhibit both physical and chemical adsorption. Ethinylquinoxaline derivatives reduce the rates of cathodic and anodic reactions, and practically do not change the polarizability and mechanism of the processes. A good correlation of efficiency with the calculated parameters of the molecules obtained within the scope of the density functional theory (DFT) B3LYP/3-21G has been found. The best correlation is realized between the protective effect and such calculated parameters as the dipole moment, the sum of effective charges, the energy difference, hardness and softness. The best in this series of inhibitors is 2,3-bis((4-methoxyphenyl)ethynyl)quinoxaline. Compound II is characterized by the highest values of the dipole moment, energy difference and softness, as well as lower values of the sum of effective charges and hardness. It has been shown that the correlation coefficients of the linear relationships “protective effect–calculated characteristics” decrease with an increase in temperature.

Received: February 7, 2025. Published: March 5, 2025 doi: 10.17675/2305-6894-2025-14-1-16

Keywords: *acid corrosion, inhibitor, ethynylquinoxaline derivatives, quantum chemical calculation.*

Introduction

Nitrogen-containing organic compounds are often studied as inhibitors of hydrochloric acid corrosion of steel. Nitrogen is included in the compounds both as a heteroatom in cycles and as a substituent in the form of amino, nitro or amide groups. In most cases, its presence

increases the inhibitory efficiency of the compound against steel corrosion. This is due to better adsorption of compounds and the formation of surface complexes with iron [1–10]. No less important is the formation of a protective polymer film on the metal surface. In this regard, when selecting possible inhibitors, researchers pay attention to the presence of multiple bonds in the compounds. High protective properties of unsaturated organic compounds, including derivatives of the propargyl series, have been shown [10–14].

The protective effect of organic compounds against metal corrosion significantly depends on their chemical structure. In recent years, the number of works has been growing in which researchers associate the effectiveness of inhibitors with the main parameters of quantum-chemical calculations. It has been repeatedly shown that the effectiveness of corrosion inhibitors is in good agreement with such calculation parameters as the dipole moment, the energy of the highest occupied and lowest free molecular orbitals, the energy difference, electronegativity, hardness, softness, *etc.* Works have appeared in which the quantum calculation of the parameters of organic molecules precedes the synthesis of compounds and testing their protective properties during metal corrosion [15, 16].

In this work, the protective effect of 2-chloro-3(*p*-tolylethynyl)quinoxaline (**I**), 2,3-bis((4-methoxyphenyl)ethynyl)quinoxaline (**II**), 2-(4-methoxyphenyl)-3-(*p*-tolylethynyl)-quinoxaline **(III**) and 2,3-bis(phenylethynyl)quinoxaline (**IV**) on the corrosion of mild steel in hydrochloric acid was studied and their efficiency was compared with the calculated parameters of the molecules.

Experimental

The synthesis of ethinylquinoxaline derivatives was described earlier [17]. The protective properties of the compounds (Tables 1, 2) in a concentration range of 10^{-5}–10^{-4} mol/l toward the corrosion of low-carbon steel in 1 M hydrochloric acid solution were compared.

Table 1. Formula, name and molar mass of the organic compounds.

Formula and name of the compound		*M*, g/mol
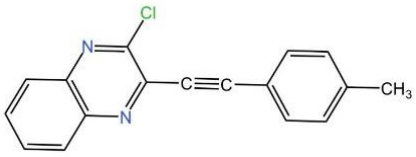	2-chloro-3(*p*-tolylethynyl)quinoxaline (I)	278
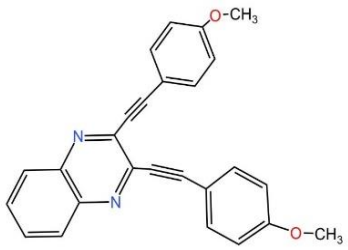	2,3-bis((4-methoxyphenyl)ethynyl)quinoxaline (II)	406

Formula and name of the compound	*M*, g/mol
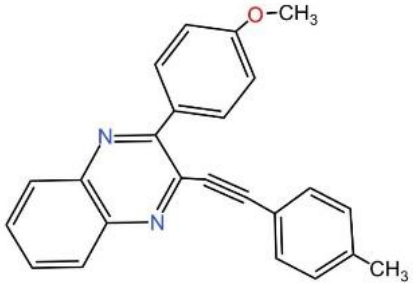 2-(4-methoxyphenyl)-3-(*p*-tolylethynyl)quinoxaline (III)	366
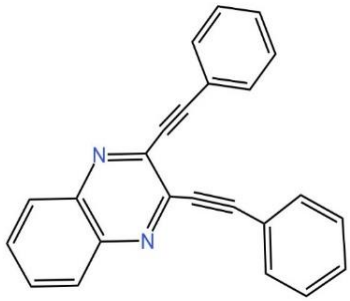 2,3-bis(phenylethynyl)quinoxaline (IV)	346

Table 2. Geometry of optimized molecules and some of their characteristics.

(I)

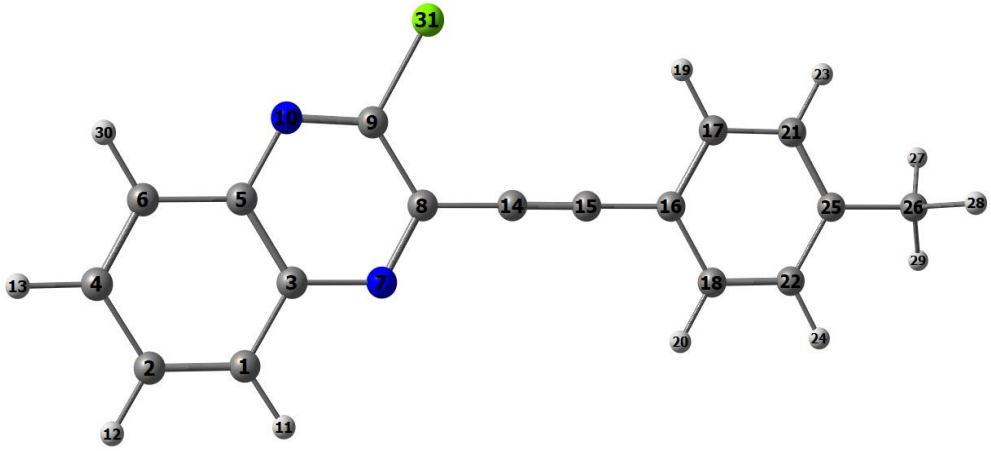

Main Atomic Distances (Å)				Main Atomic Charges			
C–N (3–7)	1.372	C–N (8–7)	1.337	(3) C	0.283498	(5) C	0.256063
C–N (5–10)	1.381	C–N (9–10)	1.290	(7) N	–0.591989	(8) C	0.223686
C–C (3–5)	1.426	C–C (8–9)	1.437	(9) C	–0.027807	(10) N	–0.563372
C–Cl (9–31)	1.843	C–C (8–14)	1.412	(14) C	0.021992	(15) C	–0.016836
C–C (15–16)	1.419	C≡C (14–15)	1.213	(16) C	–0.071281	(15) C	0.205915

Table 2 (continued). Geometry of optimized molecules and some of their characteristics.

(II)

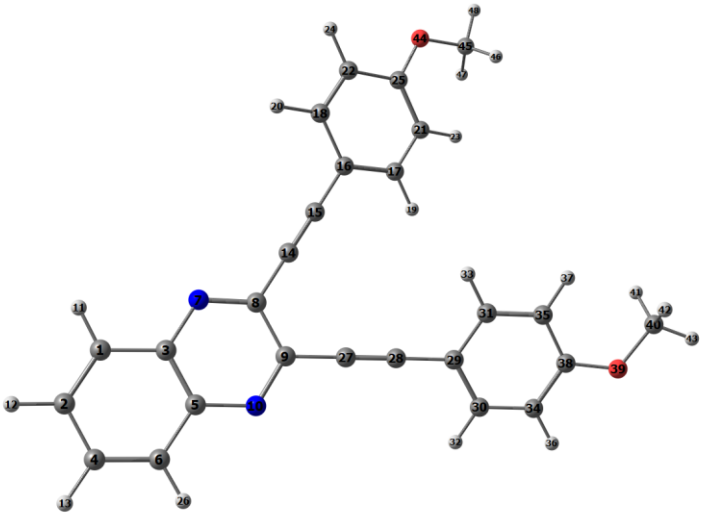

Main Atomic Distances (Å)				Main Atomic Charges			
C–N (3–7)	1.372	C–N (8–7)	1.333	(3) C	0.275784	(5) C	0.275788
C–N (5–10)	1.381	C–N (9–10)	1.333	(7) N	–0.611589	(8) C	0.229901
C–C (3–5)	1.425	C–C (8–9)	1.454	(9) C	0.229888	(10) N	–0.611592
C–C (8–14)	1.417	C–C (15–16)	1.419	(14) C	0.019831	(15) C	–0.030980
C≡C (14–15)	1.213	C–C (9–27)	1.417	(16) C	–0.068405	(27) C	0.019827
C–C (28–29)	1.419	C≡C (27–28)	1.213	(28) C	–0.030970	(29) C	–0.068411
C–O (25–44)	1.380	C–O (45–44)	1.461	(39) O	–0.566197	(44) O	–0.566196
C–O (38–39)	1.380	C–O (40–39)	1.461				

Table 2 (continued). Geometry of optimized molecules and some of their characteristics.

(III)

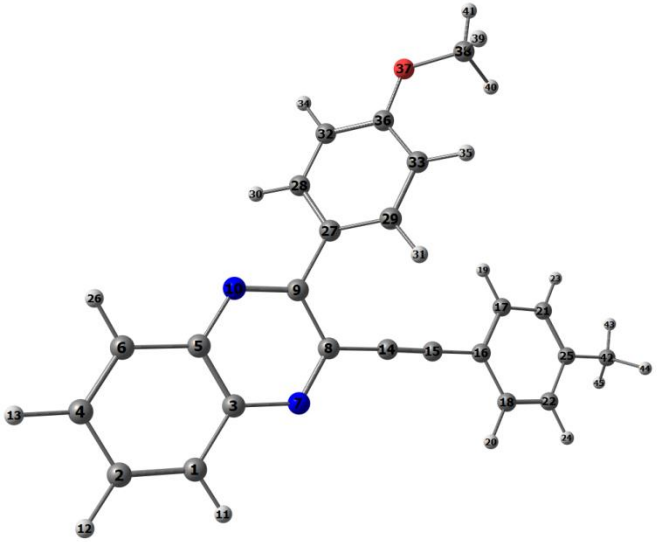

Main Atomic Distances (Å)				Main Atomic Charges			
C–N (3–7)	1.368	C–N (8–7)	1.337	(3) C	0.278517	(5) C	0.267851
C–N (5–10)	1.369	C–N (9–10)	1.332	(7) N	–0.606699	(8) C	0.163954
C–C (3–5)	1.423	C–C (8–9)	1.452	(9) C	0.302659	(10) N	–0.633202
C–C (8–14)	1.422	C–C (15–16)	1.421	(14) C	0.031676	(15) C	–0.011574
C≡C (14–15)	1.214	C–O (36–37)	1.382	(16) C	–0.071048	(36) C	0.329181
C–O (38–39)	1.460			(37) O	–0.567662	(38) C	–0.317481

Table 2 (continued). Geometry of optimized molecules and some of their characteristics.

(IV)

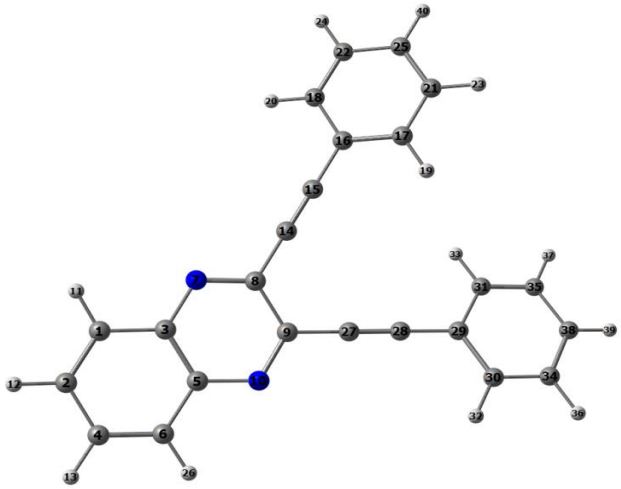

Main Atomic Distances (Å)				Main Atomic Charges			
C–N (3–7)	1.372	C–N (8–7)	1.332	(3) C	0.276915	(5) C	0.276914
C–N (5–10)	1.372	C–N (9–10)	1.332	(7) N	–0.608764	(8) C	0.230092
C–C (3–5)	1.425	C–C (8–9)	1.453	(9) C	0.230094	(10) N	–0.608766
C–C (8–14)	1.419	C–C (15–16)	1.422	(14) C	0.019686	(15) C	–0.024430
C≡C (14–15)	1.213	C–C (9–27)	1.419	(16) C	–0.056131	(27) C	0.019688
C–C (28–29)	1.422	C≡C (27–28)	1.213	(28) C	–0.024435	(29) C	–0.056132

Sample preparation and measurement methodology

In this work we used St3 steel containing 0.1–0.7% C and no more than the following amounts of other elements: 0.8% Mn, 0.4% Si, 0.05% P, 0.05% S, 0.5% Cu, 0.3% Cr, 0.3% Ni, 97% Fe. Samples $0.2 \cdot 1$ cm^2 in size for impedance measurements, 0.5×1 cm^2 in size for polarization measurements, and 1×2.5 cm^2 in size for corrosion measurements were cut from mild steel. The electrodes were cleaned with abrasive sandpaper, degreased in alcohol, washed with distilled water, and dried with filter paper. The working electrolyte

was 1 M hydrochloric acid solution. Gravimetric measurements were carried out at temperatures of 25, 40, 60 and 80°C.

The corrosion rate K was calculated by formula (1):

$$K = \Delta m \ / (\tau \cdot S) \quad (1)$$

where Δm is the mass change (grams), τ–experiment time (hours), and S is the sample area (m^2).

The efficiency of the additives was estimated by the inhibition coefficient γ (2) and the degree of protection Z (3):

$$\gamma = \frac{K_0}{K_i} \quad (2)$$

$$Z = \frac{(K_0 - K_i)}{K_0} \cdot 100\% \quad (3)$$

where K_0 and K_i are the corrosion rates in the pure acid and in the presence of an inhibitor, respectively.

Polarization measurements were carried out using an R-20X potentiostat-galvanostat (Elins Ltd., Russia) in a three-electrode thermostatically controlled cell at 25°C. A platinum counter electrode and a saturated silver chloride reference electrode were used. The potentials E are reported relative to the latter. Polarization curves were taken at a scan rate of 2 mV/s from the smaller $E = -0.7$ V to the larger $E = -0.3$ V. Each curve was reproduced in triplicate, then the results were averaged.

Capacitance measurements were carried out on a Z-500 impedance meter (Elins LLC, Russia) in a two-electrode cell in the frequency range from 1 Hz to 300 kHz at the corrosion potential. A cylindrical platinum electrode served as the auxiliary electrode ($S = 38$ cm^2). The degree of coverage of the electrode surface was calculated by the formula:

$$\Theta = \frac{S_0 - S_i}{S_0} \quad (4)$$

where S_0 and S_i are the double electric layer (DEL) capacitances in the acid solution in the absence and in the presence of inhibitors, respectively.

Quantum-chemical calculations were performed in the framework of density functional theory (DFT) B3LYP/3-21G using Gaussian09 program [17]. Geometry optimization was carried out without symmetry constraints. The DFT minima were characterized by the absence of imaginary frequencies of the calculated normal oscillations. The presented structures are obtained as a result of full optimization of all parameters and correspond to proven minimum points on the corresponding energy surfaces (PES). The electron density distribution was performed according to the Milliken scheme. The ChemCraft program [18] was used to visualize the results.

Results and discussion

The studied new derivatives of ethynylquinoxaline differ in structure. It is convenient to conduct an initial qualitative comparison of the influence of chemical structure on protective efficiency in pairs. The first pair is substances I and III containing one triple bond, the second is III and IV with two multiple bonds, Table 1. The differences in structure between the compounds of the first pair of substances consist in different substituents in position 2 of ethynylquinoxaline. In the first compound, this is an electron-acceptor substituent (chlorine), in the third, an electron-donor (4-methoxyphenyl). Accordingly, the differences in compounds II and IV consist in the presence of methoxy groups in the phenyl radicals of the second compound. These differences should be reflected in the efficiency and theoretical design parameters of the inhibitors.

The results of gravimetric measurements carried out at a temperature of 25°C are presented in Table 3.

Table 3. Dependence of the inhibition coefficient and degree of protection on the concentration and nature of additives

Inhibitor	Values of γ and *Z* (%) for $C \cdot 10^5$, mol/l									
	1.25		2.5		5		7.5		10	
	γ	*Z*	γ	*Z*	γ	*Z*	γ	*Z*	γ	*Z*
I	3.17	68.45	4.34	76.96	4.99	79.96	6.45	84.50	10.29	90.28
II	6.19	83.85	8.28	87.92	10.05	90.5	10.43	90.41	12.38	91.92
III	2.44	59.09	3.92	74.46	6.17	83.78	7.85	87.26	9.29	89.23
IV	2.28	56.07	2.54	60.67	3.65	72.62	4.17	76.03	5.54	81.94

It should be noted that the presence of different substituents in position 2 of the first pair does not significantly affect the inhibitory ability of compounds I and III. The protective effect of the first compound is somewhat higher at low and highest concentrations (C), in the region of medium C, compound III is more effective. The introduction of methoxy groups in position 4 of phenyl radicals increases the steel corrosion inhibition coefficient (compounds II and IV) by 2.5–3 times, Table 3. The best steel corrosion inhibitor is compound II, providing protection by 83.85–91.92% in the studied concentration range. Despite the presence of two multiple bonds, compound IV is inferior in efficiency to all the studied ethynylquinoxaline derivatives.

Let us compare the experimental efficiency with the calculated parameters of the compounds. The calculated characteristics of the studied molecules are presented in Table 4.

Table 4. Calculated parameters of molecules.

Inhibitor	E_{HOMO}, eV	E_{LUMO}, eV	μ, D	Σ*ED*	Δ*E*, eV	χ	η	σ
I	–6.208	–2.392	2.5687	–0.2801	–3.816	4.3	1.908	0.524109
II	–5.599	–1.986	5.3962	–1.5033	–3.613	3.7925	1.8065	0.553557
III	–5.69	–1.993	3.2018	–0.8338	–3.697	3.8415	1.8485	0.540979
IV	–6.059	–2.178	1.6688	–0.3253	–3.881	4.1185	1.9405	0.515331

Figure 1 shows the correlation coefficients of the γ–*X* linear plots, where *X* is a calculated characteristic from Table 4.

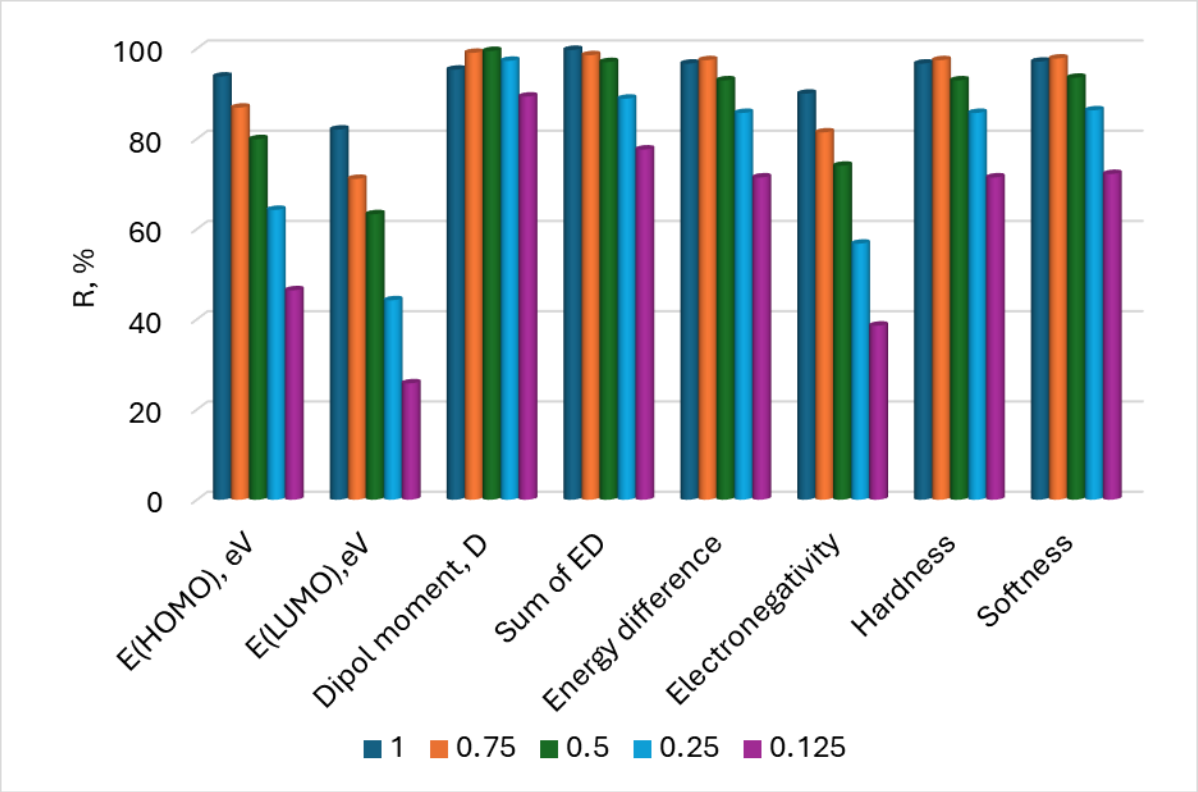

Figure 1. Correlation coefficients for the γ–*X* plots at a temperature of 25°C as a function of the concentration of compounds, $C \cdot 10^4$ mol/l.

There is a good correlation (71–99%) between the efficiency of the additives and the calculated parameters of the molecules, such as: dipole moment, sum of effective charges, energy difference, hardness and softness, Figure 1. The best in this series of inhibitors is compound II, which is characterized by the highest values of the dipole moment, energy difference and softness, as well as lower values of the sum of effective charges and hardness.

It should be noted that with increasing temperature, both the protective effect of additives and its correlation with the calculated parameters of molecules decrease (47.8-54.7% at 80°C). Obviously, the inhibitor film is not dense enough and polymerization

of compounds on the steel surface does not occur. This assumption is confirmed by the decrease in the protective effect of inhibitors with increasing temperature, Figure 2.

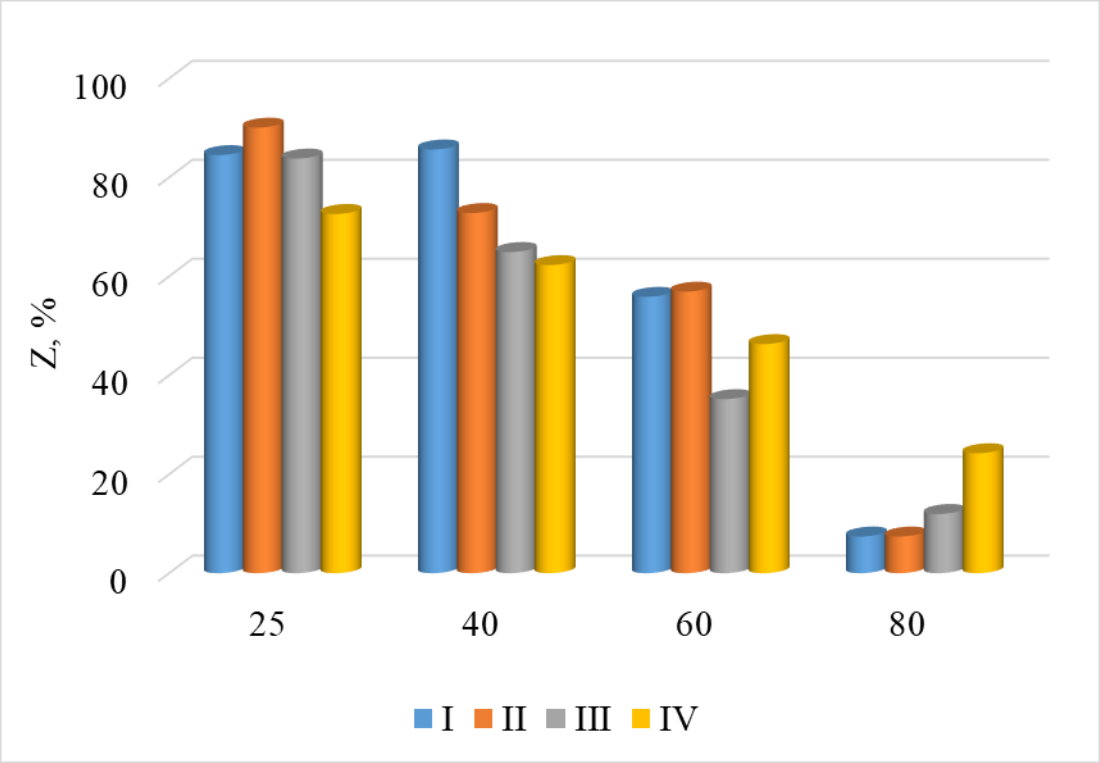

Figure 2. Dependence of the inhibition degree on temperature and nature of the compound at a concentration of C=0.1 mmol/l.

At 60°C, the protective effect of the compounds is only 35–56%. At the same time, all compounds increase the value of the effective activation energy (E_a) of the corrosion process compared to E_a, which is observed in acid without an inhibitor, by 14–34 kJ/mol, Table 5.

Table 5. Values of θ, E_a, ΔG_{ads} and correlation coefficients (R) of the corresponding linear dependencies for their calculation

Inhibitor	E_a, kJ/mol	R, %	$-\Delta G$, kJ/mol	R, %	θ, %
I	94.2	99.4	41.3	99.9	40.3
II	106.1	98.9	44.1	99.9	44.8
III	89.3	98.7	38.9	99.5	45.2
IV	86.6	98.5	38.4	99.9	47.8

Analysis of the concentration dependence of efficiency at a temperature of 25°C showed that the adsorption of the studied compounds is described by the Langmuir isotherm, which is characteristic of a homogeneous surface. The free adsorption energy of compounds (ΔG_{ads}) was calculated using equation:

$$\Delta G_{ads} = -RT \ln(55.55 \cdot B) \quad (5)$$

where R is the universal gas constant, T is the temperature, and B is the adsorption constant.

Compounds I and II are characterized by only chemical adsorption ($\Delta G_{ads} < -40$ kJ/mol); in the case of the other compounds, both physical and chemical adsorption occur (-20 kJ/mol $< \Delta G_{ads} < -40$ kJ/mol).

The Nyquist plots obtained for steel in solutions of hydrochloric acid without and with the additives have a qualitatively similar appearance (Figure 3).

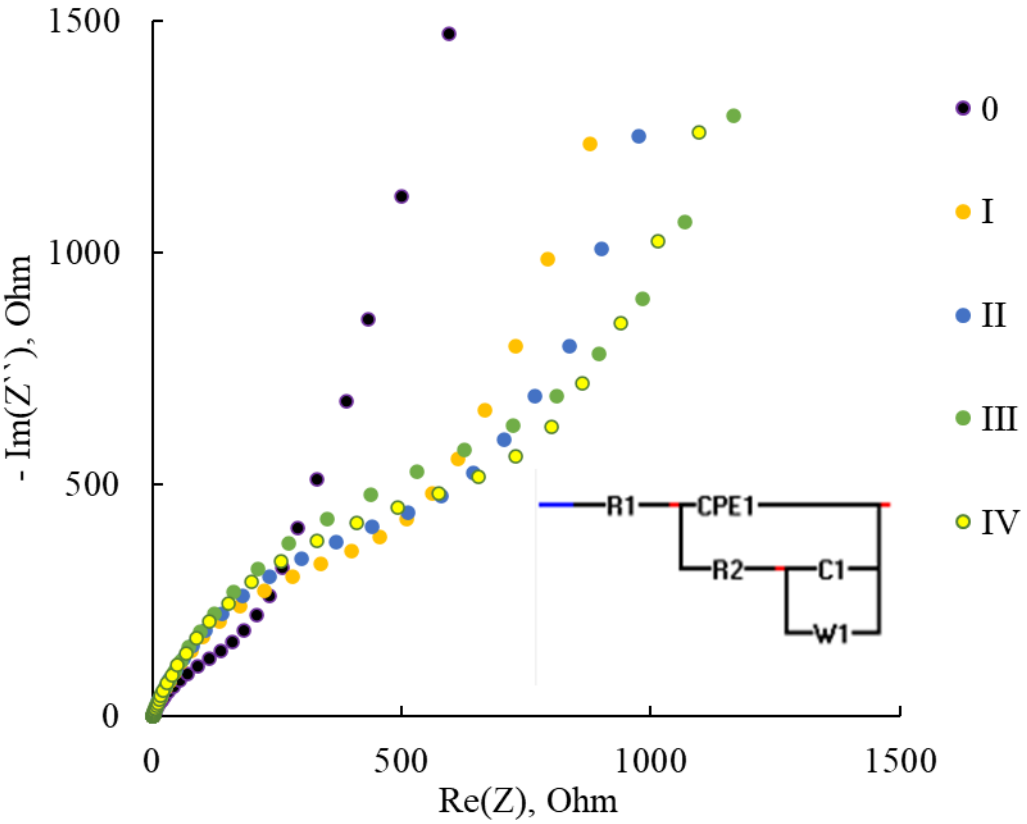

Figure 3. Nyquist plots of steel in 1 M HCl solution without inhibitors (0) and in the presence of inhibitors I, II, III and IV at C = 0.05 mmol/l.

Using the selected equivalent circuits, the DEL capacitance was determined and the degrees of surface coverage (θ) with the inhibitors were calculated using formula (4), Table 5. The degree of surface coverage is smaller than the degree of protection at all concentrations, Tables 3, 5. This indicates a mixed mechanism of the protective action of these inhibitors.

The polarization curves obtained on steel in the hydrochloric acid solution without (0) and in the presence of inhibitors have a qualitatively similar appearance, Figure 4.

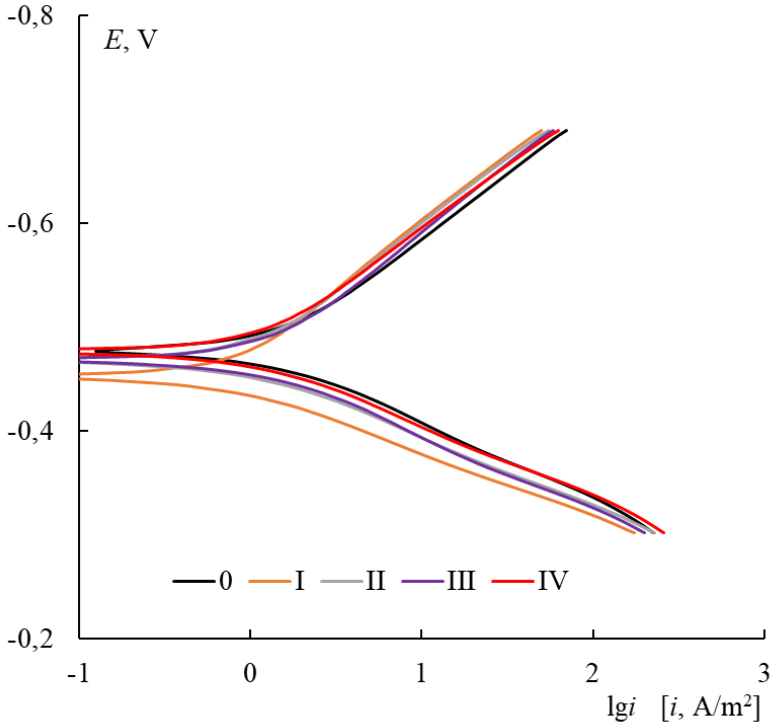

Figure 4. Polarization curves of steel in hydrochloric acid solution without (0) and in the presence of inhibitors (I–IV) at C = 0.05 mmol/l.

All compounds are mixed type inhibitors. Compound I mainly inhibits steel dissolution. All inhibitors practically do not change the polarizability of the cathode and anodic reactions, which indicates the constancy of the mechanism of the processes taking place, Figure 4.

Conclusion

Thus, the studied ethynylquinoxane derivatives are mixed type inhibitors. They reduce the rate of steel corrosion in hydrochloric acid by blocking part of the surface and increasing the effective activation energy of the process. A good correlation of efficiency with the calculated characteristics of the molecules is realized.

References

1. N.P. Andreeva, D.S. Kuznetsov, Ya.G. Avdeev, Investigation of the adsorption of IFKHAN-92 inhibitor on the surface of chromium-nickel steel from hydrochloric and sulfuric acid solutions by ellipsometry, *Korroz.: Mater., Zashch, (Corrosion: Materials, Protection)*, 2018, no. 2, 18–24 (in Russian).
2. Ya.G. Avdeev, D.S. Kuznetsov, Yu.B. Makarychev and L.P. Kazansky, Protective aftereffect of IFKHAN-92 inhibitor in case of corrosion of chromium-nickel steel in hydrochloric acid, *Korroz.: Mater., Zashch. (Corrosion: Materials, Protection)*, 2019, no. 4, 20–25 (in Russian). doi: 10.31044/1813-7016-2019-0-4-20-25

3. Yu.I. Kuznetsov, Triazoles are a class of multifunctional corrosion inhibitors, Overview, Part II. 1,2,3-benzotriazole and its derivatives. Iron and steel, *Korroz.: Mater., Zashch. (Corrosion: Materials, Protection)*, 2020, no. 8, 3–22 (in Russian). doi: 10.31044/1813-7016-2020-0-8-3-22
4. M.D. Plotnikova, A.B. Shein and A.E. Rubtsov, Adsorption and protective properties of a number of thiazole and thiadiazole derivatives on low-carbon steel in hydrochloric acid solution, *Korroz.: Mater., Zashch. (Corrosion: Materials, Protection)*, 2021, no. 7, 19–26 (in Russian). doi: 10.31044/1813-7016-2021-0-7-19-26
5. H. Bouammali, F. Abrigach, S. Jerdioui, B. El-Haitout, A. Aouniti, R. Touzani, B. Hammouti and R. Salghi, Effect of the addition of two pyrazole derivatives on behavior of the corrosion of mild steel in a 1 M HCl medium using experimental and theoretical insights, *Int. J. Corros. Scale Inhib.*, 2024, **13**, no. 1, 367–396. doi: 10.17675/2305-6894-2024-13-1-19
6. M.H. Abdulkareem, Z.A. Gbashi, B.A. Abdulhussein, M.M. Hanoon, A.A.H. Kadhum, A.A. Alamiery and W.K. Al-Azzawi, Investigating the corrosion inhibitory properties of 1-benzyl-4-imidazolidinone on mild steel in hydrochloric acid: a thorough experimental and quantum chemical study, *Int. J. Corros. Scale Inhib.*, 2024, **13**, no. 1, 411–434. doi: 10.17675/2305-6894-2024-13-1-21
7. M.T. Mohamed, A.N. Jasim, S.A. Nawi, A.M. Mustafa, F.F. Sayyid, A.A. Khadom, A.A. Alamiery, A.A.H. Kadhum and T.S. Gaaz, Performance of 4-methyl-2-(1-aminoethyl)-1,3-thiazole in mitigating mild steel corrosion in hydrochloric acid, *Int. J. Corros. Scale Inhib.*, 2025, **14**, no. 1, 109–131. doi: 10.17675/2305-6894-2025-14-1-7
8. M. Bouziani Idrissi, H. Hailou, I. Filali, M. Rbaa, F. Benhiba, K. Nouneh, E.El Kafsaoui, C. El Mahjoub, A. El Midaoui, H. Oudda and A. Zarrouk, Theory and experimental investigations on the effect of the halogenated chain of new synthesis compounds based on benzimidazole derivatives on the inhibition corrosion of mild steel in acid media, *Int. J. Corros. Scale Inhib.*, 2023, **12**, no. 4, 1535–1563. doi: 10.17675/2305-6894-2023-12-4-8
9. A. Elbarki, Z. Amrani, T. Laabaissi, M. El Faydy, L. Adlani, A. Fatah, F. Benhiba, M. Rbaa, I. Warad, B. Lakhrissi, H. Zarrok, A. Bellaouchou, B. Dikici, H. Oudda and A. Zarrouk, The inhibitory effect of certain imidazole derivatives grafted on 8-hydroxyqinoline on carbon steel corrosion in acidic medium: experimental and computational approaches, *Int. J. Corros. Scale Inhib.*, 2023, **12**, no. 3, 1292–1320. doi: 10.17675/2305-6894-2023-12-3-27
10. B.S. Mahdi, H.S.S. Aljibori, M.K. Abbass, W.K. Al-Azzawi, A.H. Kadhum, M.M. Hanoon, W.N.R.W. Isahak, A.A. Al-Amiery and H.Sh. Majdi, Gravimetric analysis and quantum chemical assessment of 4-aminoantipyrine derivatives as corrosion inhibitors, *Int. J. Corros. Scale Inhib.*, 2022, **11**, no. 3, 1191–1213. doi: 10.17675/2305-6894-2022-11-3-17

11. M.G. Veliyev, M.I. Shatirova, G.D. Heydarova and F.M. Aliyeva, Amino-containing acetylenes are inhibitors of acid corrosion of steel, *Korroz.: Mater., Zashch. (Corrosion: Materials, Protection)*, 2016, no. 5, 22–26 (in Russian).
12. M.I. Shatirova and Ya.G. Avdeev, The effect of phosphorus-containing esters of the propargyl series on corrosion of steel in hydrochloric acid, *Korroz.: Mater., Zashch. (Corrosion: Materials, Protection)*, 2016, no. 11, 34–39 (in Russian).
13. Ya.G. Avdeev and Yu.I. Kuznetsov, High-temperature corrosion of steels in acid solutions. Pt. 2. Inhibitory protection of steels with unsaturated organic compounds, *Korroz.: Mater., Zashch. (Corrosion: Materials, Protection)*, 2020, no. 10, 1–19 (in Russian). doi: 10.31044/1813-7016-2020-0-10-1-19
14. O.Y. Grafov and L.P. Kazansky, Porphyrins, phthalocyanines and their derivatives as metal corrosion inhibitors, *Korroz.: Mater., Zashch. (Corrosion: Materials, Protection)*, 2020, no. 9, 1–10 (in Russian). doi: 10.31044/1813-7016-2020-0-9-1-10
15. R.K. Mitra, R. Yadav, A. Tomar and M. Yadav, Computational and experimental evaluation on pyrazoles as corrosion inhibitor in HCl solution: DFT and electrochemical analysis, *Int. J. Corros. Scale Inhib*., 2024, **13**, no. 4, 1908–1935. doi: 10.17675/2305-6894-2024-13-4-2
16. D.V. Lyapun, A.A. Kruzhilin, D.S. Shevtsov and Kh.S. Shikhaliev, Investigation of the inhibitory activity of some 3-aryl(hetaryl)-5-amino-1*H*-1,2,4-triazoles on copper chloride corrosion, *Int. J. Corros. Scale Inhib*., 2024, **13**, no. 2, 874–891. doi: 10.17675/2305-6894-2024-13-2-12
17. A.V. Gulevskaya, E.A. Shvydkova and D.I. Tonkoglazova, Synthesis and Characterization of Pyridine-, Pyrazine- and Quinoxaline-derived [4]Helicenes and S-Shaped Double [4]Helicenes, *Eur. J. Org. Chem*., 2018, **36**, 5030–5043. doi: 10.1002/ejoc.201800613
18. *Gaussian 09, Revision A.02*, M.J. Frisch, G.W. Trucks, H.B. Schlegel, G.E. Scuseria, M.A. Robb, J.R. Cheeseman, G. Scalmani, V. Barone, B. Mennucci, G.A. Petersson, H. Nakatsuji, M. Caricato, X. Li, H.P. Hratchian, A.F. Izmaylov, J. Bloino, G. Zheng, J.L. Sonnenberg, M. Hada, M. Ehara, K. Toyota, R. Fukuda, J. Hasegawa, M. Ishida, T. Nakajima, Y. Honda, O. Kitao, H. Nakai, T. Vreven, J.A. Montgomery, Jr., J.E. Peralta, F. Ogliaro, M. Bearpark, J.J. Heyd, E. Brothers, K.N. Kudin, V.N. Staroverov, R. Kobayashi, J. Normand, K. Raghavachari, A. Rendell, J.C. Burant, S.S. Iyengar, J. Tomasi, M. Cossi, N. Rega, J.M. Millam, M. Klene, J.E. Knox, J.B. Cross, V. Bakken, C. Adamo, J. Jaramillo, R. Gomperts, R.E. Stratmann, O. Yazyev, A.J. Austin, R. Cammi, C. Pomelli, J.W. Ochterski, R.L. Martin, K. Morokuma, V.G. Zakrzewski, G.A. Voth, P. Salvador, J.J. Dannenberg, S. Dapprich, A.D. Daniels, Ö. Farkas, J.B. Foresman, J.V. Ortiz, J. Cioslowski and D.J. Fox, *Gaussian*, Inc., Wallingford CT, 2009.
19. https://www.chemcraftprog.com

♦ ♦ ♦